Green Chemistry

PAPER

View Article Online
View Journal | View Issue

Cite this: *Green Chem.*, 2014, **16**, 4566

A recoverable Pd nanocatalyst for selective semi-hydrogenation of alkynes: hydrogenation of benzyl-propargylamines as a challenging model†

Paula M. Uberman,[a] Natalia J. S. Costa,[a] Karine Philippot,[b,c] Rafaela C. Carmona,[d] Alcindo A. Dos Santos[d] and Liane M. Rossi*[a]

Received 12th April 2014,
Accepted 20th July 2014

DOI: 10.1039/c4gc00669k

www.rsc.org/greenchem

We describe a recyclable heterogeneous palladium nanocatalyst for the selective hydrogenation of alkynes to alkenes. The catalyst was prepared through the decomposition of the organometallic precursor $Pd_2(dba)_3$ over a magnetic support, obtaining well-dispersed Pd nanoparticles that formed exclusively on the support surface, with average diameter of 3.5 ± 0.8 nm. The catalytic activity was investigated in the hydrogenation reactions of alkenes and alkynes, and the chemo- and stereoselectivity were evaluated in the hydrogenation of benzyl-propargylamines. The catalyst is highly selective in performing semi-hydrogenation reactions under mild conditions and short reaction times, with good overall yields. Furthermore, it can be easily recovered and recycled, with no leaching of palladium detected, and activities and selectivity retained over multiple reaction cycles.

Introduction

Hydrogenation reactions are considered one of the most valuable synthetic transformations in organic chemistry. In particular, the selective semi-hydrogenation of alkynes to obtain alkenes is a challenging task in organic synthesis, and it is an important reaction in the chemical industry.[1] Selective palladium catalysts are usually promoted by a second metal, for example the Lindlar catalyst comprised of $Pd/CaCO_3$ partially poisoned with lead. Catalyst deactivation and the presence of toxic lead are the main drawbacks for the utilization of this catalyst system in true green processes. In addition, there is a growing demand for transformations of highly functionalized molecules to prepare complex molecules in fine chemical production. In this sense, the synthesis and modification of propargylamines have gained popularity in recent years due to their applications in the synthesis of natural products and pharmaceutical compounds.[2–6] Propargylamine derivatives can be synthesized using several approaches, such as the addition of aryl- and alkylacetylene derivatives to imines[7,8] or enamines,[9,10] cross-dehydrogenative-coupling (CDC),[11] or the decarboxylation-coupling of secondary amino acids.[12] In addition to these methods, the A^3 coupling reaction, a multicomponent reaction of an aldehyde, an amine, and an alkyne, has received attention for its practicality.[13] It is possible to obtain, in a single step, propargylamines substituted with several functional groups with good yield. Propargylamines are important intermediates in the synthesis of alkaloids, amino acids, and nitrogen heterocycles.[14,15] Several steps of hydrogenation could be necessary for the transformation of propargylamines into the target molecules, and usually only the fully hydrogenated product is obtained.[7,10,16,17] When benzylamines are used, the hydrogenation process becomes challenging, as it could lead to a debenzylated product, leaving the amino group unprotected.[10,18] Therefore, the development of a highly active and selective catalyst to perform alkyne hydrogenation, as well as the more demanding hydrogenation of propargylamines, is an area of current interest.

Pd-catalyzed reactions of pharmaceutically active ingredients may have problems associated with the retention of Pd (and metal promoters) in the final product. There is a strict limit for the levels of heavy metals in a drug substance.[19] The preparation of catalysts, especially lead-free Pd catalysts, in which the leaching of metals can be minimized is highly relevant to the development of green chemical processes, providing significant advantages in the safe production of organic compounds. Functionalized magnetic nanoparticles (MNPs)

[a]*Laboratory of Nanomaterials & Catalysis, Institute of Chemistry, Universidade de São Paulo, Av. Professor Lineu Prestes, 748, São Paulo 05508-000 SP, Brazil. E-mail: lrossi@iq.usp.br*
[b]*CNRS, LCC (Laboratoire de Chimie de Coordination), 205, route de Narbonne, F-31077 Toulouse cedex 4, France*
[c]*Université de Toulouse, UPS, INPT, LCC, F-31077 Toulouse, France*
[d]*Laboratory of Organocatalysis and Organic Synthesis, Institute of Chemistry, Universidade de São Paulo, Av. Professor Lineu Prestes, 748, São Paulo 05508-000 SP, Brazil*

†Electronic supplementary information (ESI) available: Characterization data and NMR spectroscopy. See DOI: 10.1039/c4gc00669k

have emerged as options to facilitate catalyst recovery.[20] They offer the advantage of being magnetically separable, thereby eliminating the requirement of catalyst filtration after completion of the reaction and avoiding the exposure of the catalyst to air during the recycling, which are important and desired characteristics in the field of organic synthesis.

Noble metal nanoparticles with high specific catalytic activity are ubiquitous in modern synthetic organic chemistry,[21] and hydrogenation reactions are not an exception. Recently, a variety of magnetically recoverable metal nanocatalysts have been studied in the hydrogenation of alkynes with variable results.[22–25] Fe-based nanocatalysts exhibit good activity but low selectivity to the alkene product.[23,24] Alper *et al.* prepared Pt nanoparticles supported on MNPs modified with ionic liquids (ILs),[25] and they exhibited a very high activity and selectivity for (*Z*)-alkene in the hydrogenation of diphenylacetylene under harsh reaction conditions (90 °C, 200 psi H_2, and 16 hours). Conversely, Scott *et al.*[26] synthesized Pd nanoparticles supported on MNPs stabilized by tetraalkylphosphonium ILs, but they showed a very low selectivity for the alkene in the hydrogenation of 3-hexyn-1-ol. Under the best conditions, the alkene was obtained with a 41% yield, whereas 59% of the hexanol was produced. Despite this, Pd nanoparticles supported on magnetic carriers still remain largely unexplored in selective hydrogenations. Moreover, most of the catalytic studies were performed with simple or less functionalized alkynes.

Several methods have been established for the synthesis of metallic nanoparticles with high control of the size and morphology, including the use of physical techniques, such as atom evaporation, and techniques based on salt reduction or compound precipitation, as well as electrochemical synthesis, the use of micelles as nanoreactors, and the organometallic approach. The decomposition of metal(0) organometallic compounds in the presence of a stabilizing agent in organic media was reported by Chaudret and Philippot as an innovative strategy for synthesizing metal nanoparticles.[27,28] This methodology allowed the preparation of metal nanoparticles under very mild conditions (room temperature, low gas pressure) with the additional advantage of precise control of the surface of the nanoparticles, in particular the absence of oxidation and the number and nature of surface species (ligands). Based on the advantages of using organometallic precursors, our research group developed the preparation of supported nanocatalysts through the direct decomposition of the organometallic precursor over silica-coated MNP. Highly active and magnetically recoverable Ni[29] and Pd[30] nanocatalysts were prepared by decomposition of [$Ni(cod)_2$ and $Pd_2(dba)_3$]. We also demonstrated that the co-decomposition of such precursors can be used to produce bimetallic NiPd nanoparticles of various compositions as highly active hydrogenation catalysts.[31] Later, Reiser *et al.*[32,33] also used the concept of magnetic separation (carbon-coated cobalt nanobeads) and the decomposition of $Pd_2(dba)_3$ to prepare magnetically recoverable catalysts for alkene hydrogenation. Here we have chosen to synthesize a magnetically recoverable Pd catalyst through the direct decomposition of the organometallic precursor [$Pd_2(dba)_3$] with particular interest in selective hydrogenation of propargylamines.

Results and discussion

The catalyst preparation was performed through the direct decomposition of the organometallic precursor [$Pd_2(dba)_3$] with dihydrogen in the presence of an amino-modified silica-coated magnetite nanoparticle ($FFSiNH_2$).[34] The [$Pd_2(dba)_3$] precursor decomposes easily under dihydrogen atmosphere leading to the production of Pd nanoparticles free of contaminants after the purification step.[28] In such a way, this methodology allowed us to obtain well-dispersed Pd nanoparticles formed exclusively on the support surface, with average diameter of 3.5 ± 0.8 nm (Fig. 1). The organometallic precursor was totally decomposed over the magnetic support, and no metal remained in the final solution (palladium < 0.02 ppm). The Pd loading determined by the ICP OES was 3.6 wt%. A representative transmission electron microscopy (TEM) image of the obtained nanomaterial (Fig. 1) also revealed that the core–shell nanostructured catalyst support was unchanged after palladium deposition.

The catalytic behavior of the supported Pd nanocatalyst was first tested using the well-established hydrogenation of cyclohexene as a model substrate for the hydrogenation reactions. Thus, cyclohexene was placed in a Fischer–Porter glass in the presence of 0.005 mol% catalyst, 6 bar of dihydrogen, and heated at 75 °C. The reaction was monitored by dihydrogen consumption *versus* time. Under these conditions, the turnover frequency (TOF) obtained was 40 000 $mol_{cyclohexene}\ mol_{Pd}^{-1}\ h^{-1}$ at initial rates. This value corresponds to an enhanced activity compared with a palladium catalyst prepared from $PdCl_2$ immobilized in the same support and reduced by dihydrogen.[35] However, it is difficult to precisely determine whether this increase is attributed to the effect of particle size, size distribution, and metal dispersion or the surface state of the palladium nanoparticles. Indeed it is expected that the organometallic approach leaves the metallic surface more

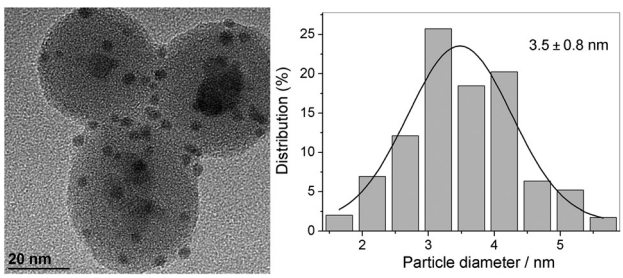

Fig. 1 TEM image of the magnetic catalyst $FFSiNH_2Pd$ prepared from [$Pd_2(dba)_3$] over the magnetic support $FFSiNH_2$.

clean and available for catalysis in comparison with the precursor $PdCl_2$, in which the chlorides contaminate the surface of the catalyst.

Afterward, we tested the activity and selectivity of the Pd catalyst in alkyne hydrogenation. In this case, 3-butyn-1-ol (**1**) was used as a model substrate (Scheme 1). This simple alkyne was chosen to evaluate and compare the catalyst selectivity for partial and full-hydrogenation products 3-buten-1-ol (**2**) and *n*-butanol (**3**).

Initially, we evaluated the effect of the solvent on the catalytic activity. Cyclohexane, toluene, dichloromethane, and ethanol were tested for the hydrogenation reaction in the presence of 0.2 mol% of Pd, at 27 °C, and 3 bar of H_2. The reaction progress was followed by H_2 pressure measurements (Fig. 2). Ethanol would be the first choice as a green and inexpensive solvent, but the reaction was too fast, and in 20 minutes the alkyne **1** was converted into the fully hydrogenated *n*-butanol (**3**) (entry 1, Table 1). The reactions performed in dichloromethane and toluene also produced only product **3** after 30 and 40 minutes, respectively (entries 2 and 3, Table 1). The reaction in cyclohexane required longer reaction times for completion (*ca.* 72 minutes), but it also produced only product **3** (entry 4, Table 1). The fully hydrogenated product **3** was obtained in all solvents, which is in agreement with the consumption of two equivalents of dihydrogen (Fig. 2). After the consumption of one equivalent of H_2, the conversion of alkyne **1** was nearly completed, and the major product was alkene **2**, obtained in 82% selectivity (entry 5, Table 1).

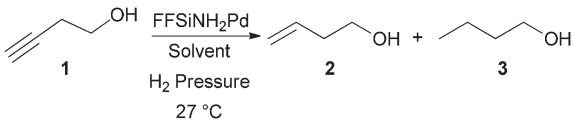

Scheme 1 Catalytic hydrogenation of 3-butyn-1-ol (**1**) with the $FFSiNH_2Pd$ nanocatalyst.

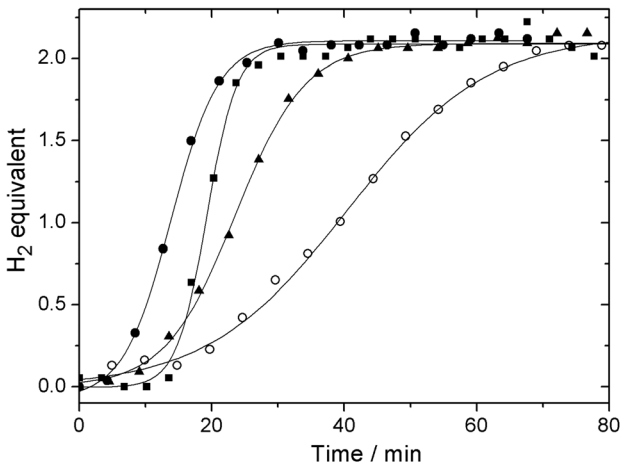

Fig. 2 Solvent evaluation in the catalytic hydrogenation of 3-butyn-1-ol with $FFSiNH_2Pd$: ethanol (circle), dichloromethane (square), toluene (triangle), and cyclohexane (open circle).

Table 1 Catalytic hydrogenation of 3-butyn-1-ol (**1**) with $FFSiH_2Pd$[a]

Entry	Solvent	Time (min)	Conv.[b] (%)	Select. (%)	Initial rate[c]	TOF[d]
1	Ethanol	25	100	**3**: 100%	9.42	2410
2	CH_2Cl_2	27	100	**3**: 100%	10.18	2907
3	Toluene	41	100	**3**: 100%	7.28	1848
4	Cyclohexane	70	100	**3**: 100%	2.58	736
5	Cyclohexane	45	98	**2**: 82% **3**: 18%		
6[e]	Cyclohexane	150	100	**2**: 68% **3**: 31%	0.63	173
7[f]	Cyclohexane	90	93	**2**: 89% **3**: 11%	2.97	7270
8[g]	Cyclohexane	480	100	**3**: 100%	1.06	287
9[g]	Cyclohexane	270	94	**2**: 27% **3**: 73%		
10[g]	Cyclohexane	120	54	**2**: 58% **3**: 42%		

[a] Reaction conditions: 1.5 mmol alkyne, ~10 mg catalyst (0.2 mol%), 5 mL solvent, 27 °C, 3 bar H_2. [b] Quantified by GC analysis. [c] Initial rate: mmol H_2 h^{-1}. [d] TOF initial: mol H_2 mol^{-1} Pd h^{-1}. [e] H_2 pressure at 1 bar. [f] The reaction was performed with 0.04 mol% Pd. [g] Reaction performed with Pd/C (0.2 mol%).

In the reaction performed at 1 bar H_2, at 100% conversion, the product composition was 68% alkene **2** and 31% of alkane **3** (entry 6, Table 1). Thus, under this condition, the catalyst was more selective than the reaction at 3 bar (entry 4, Table 1); however, 150 minutes were necessary to achieve complete conversion. When a lower catalyst loading was used (0.04 mol% Pd), 89% selectivity for the semi-hydrogenated product **2** was obtained at 93% conversion (entry 7, Table 1). The catalyst reached a high TOF value of 7270 h^{-1} at initial rates. In addition, when the reaction was performed without a Pd source, alkyne **1** was recovered without changes after 8 h of reaction. The reaction performed under similar conditions with the commercial Pd/C catalyst (3 wt%) took nearly 8 h to convert alkyne **1** into product **3** (entry 8, Table 1). When this reaction was stopped at about 4.5 h after the reaction began, the conversion of alkyne **1** reached 94%, but the major product was again the fully hydrogenated product **3**, obtained in 73% selectivity (entry 9, Table 1). At lower conversion, the fully hydrogenated product **3** was also present (entry 10, Table 1). Therefore, the $FFSiNH_2Pd$ catalyst exhibited higher activity and selectivity to perform the semi-hydrogenation of 3-butyn-1-ol than Pd/C under the studied conditions. The optimum condition for high selectivity for the semi-hydrogenated product is **3** bar of H_2, 0.04 mol% Pd and cyclohexane. In an attempt to explore the hydrogenation mechanism, a temporal evolution of the product composition was examined (Fig. 3). The hydrogenation reaction takes place exclusively on the alkyne, maintaining a high selectivity (>90% selectivity), and only after almost all of alkyne **1** was reduced the alkene hydrogenation started. This behavior suggests that the active sites of the catalyst are preferentially occupied by the alkyne, thus retarding the hydrogenation of 3-buten-1-ol (**2**). Conse-

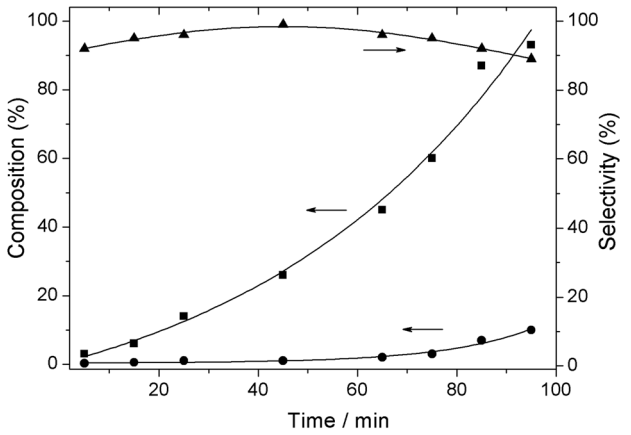

Fig. 3 Temporal evaluation of the product composition in the catalytic hydrogenation of 3-butyn-1-ol with $FFSiNH_2Pd$. Alkene (square), alkane (circle), and selectivity to alkene (triangle).

quently, in the presence of a high concentration of alkyne **1**, the binding of 3-buten-1-ol (**2**) to the catalyst is prevented until the concentration of alkyne **1** is significantly reduced to start the hydrogenation of alkene **2**. Alkynes are actually known to coordinate more strongly with the catalyst surface than the alkenes, providing high selectivity to the semi-hydrogenation reaction over modified Pd catalysts.[1,36–39] The control of the hydrogenation selectivity is usually obtained by surface poisoning when adding surface modifiers (metal, carbon, sulfur, *etc.*),[35,40,41] but Pd can also be modified under reaction conditions, not only by surface deposits, but also by sub-surface species.[42] As no extra stabilizer was added for the synthesis of the Pd nanoparticles, the most plausible catalyst modifiers are the –N donor ligands present in the amino-functionalized supports.

Next, the chemo- and steroselectivity of the catalyst $FFSiNH_2Pd$ were evaluated. For this purpose, more challenging substrates, such as propargylamine **4a–c**, were considered (Scheme 2). A series of propargylamine **4a–c** was synthesized through an A^3 coupling reaction employing 1 mol% CuCl for 12 h in ethyl acetate under 105 °C in a glass pressure reactor. The alkynes **4a–c** were obtained in one step, with 64–83% isolated yield (Scheme 2).[43]

The propargylamine **4a** (1 mmol), the catalyst $FFSiNH_2Pd$, and cyclohexane (5 mL) were charged in a Fischer–Porter glass reactor, and the hydrogenation reaction was performed at 3 bar H_2 and 27 °C. Two products were observed, the alkene **5a** and the fully-hydrogenated product **6** (Scheme 3). The reaction

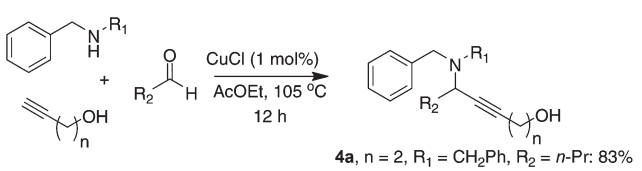

Scheme 2 Synthesis of propargylamines using an A^3 coupling reaction.

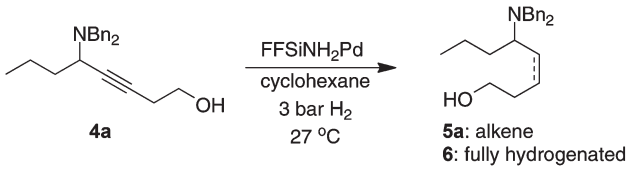

Scheme 3 Hydrogenation of propargylamine **4a** with the $FFSiNH_2Pd$ catalyst.

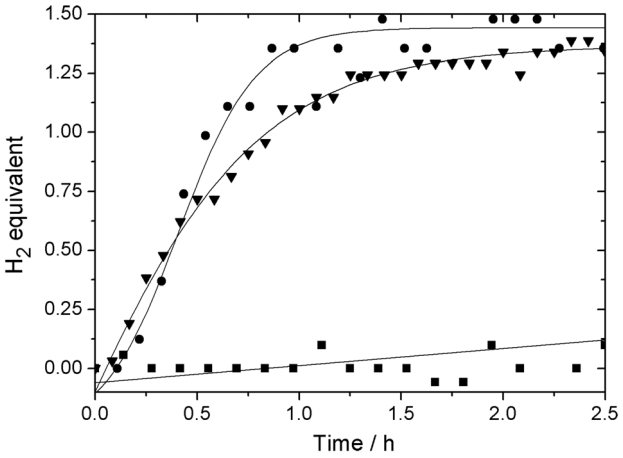

Fig. 4 Catalytic hydrogenation of propargylamine **4a** with $FFSiNH_2Pd$ (0.20 mol% (circle), 0.04 mol% (triangle)) and Pd/C (0.04 mol% (square)).

was followed by H_2 consumption (Fig. 4). The reaction proceeded very fast when 0.2 mol% of the $FFSiNH_2Pd$ was employed, and one equivalent of H_2 was consumed after 0.5 h. When a longer reaction time was allowed, after 2 h the composition of the product was 82% alkene **5a** and 18% fully hydrogenated product **6**. The product's composition remained essentially unchanged for a few hours, reaching an equilibrium point in the hydrogenation curve, as shown in Fig. 4. After 24 h, the product's composition changed slightly: 75% alkene **5a** and 25% product **6**. These results indicated that the coordination with the catalyst surface was hindered more in the case of alkene **5a**, and the alkene was forced to leave the surface; thus, the over-hydrogenation process was efficiently suppressed. Only after 24 h of reaction at 40 °C was the fully hydrogenated product **6a** obtained in 68% yield. Under lower catalyst loading conditions (0.04 mol% of Pd), propargylamine **4a** was hydrogenated in the corresponding alkene **5a** with 88% selectivity after 1.5 h (68% isolated yield). After 1 h of reaction, the H_2 consumption reached one equivalent; however, some alkyne **4a** still remained in the reaction mixture. Commercial Pd/C (3 wt%) was also examined under similar conditions, but it exhibited lower activity (Fig. 4). The reaction took more than 3 h to start. Therefore, the hydrogenation of propargylamine **4a–c** was performed with $FFSiNH_2Pd$, employing 0.04 mol% Pd. The results are summarized in Table 2. Propargylamines **4b** and **4c** showed similar reactivity to propargylamine **4a** for the hydrogenation reaction. After 2 h in the presence of 3 bar hydrogen, alkenes **5b** and **5c** were obtained in 53% and 61%

Table 2 Catalytic hydrogenation of propargylamine **4a–c** with magnetic $FFSiNH_2Pd$[a]

Entry	Substrate	Product	Conversion[b] (selectivity)	Isolated yield (%)
1	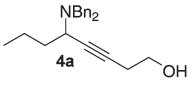 **4a**	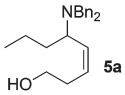 **5a**	100% (88%)	68
2	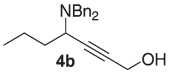 **4b**	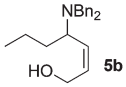 **5b**	91% (97%)	53
3	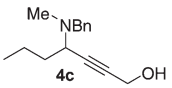 **4c**	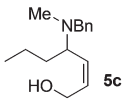 **5c**	n.d.[c]	61

[a] Reaction conditions: 1 mmol alkyne, ~2 mg catalyst (0.04 mol%), 5 mL solvent, 27 °C, 2 h, and 3 bar hydrogen atmosphere. [b] Determined by CG analysis. [c] n.d. = not determined.

isolated yields, respectively (entries 2 and 3, Table 2). In terms of stereoselectivity, when the reactions were performed under short reaction times, the main products detected by GC analysis were the alkenes **5a–c**. Under these conditions, no side reactions, such as isomerization or debenzylation, were observed. The stereochemistry of these products was studied using ^{1}H NMR analysis. The products **5b–c** correspond to the *Z*-isomers, and the configuration of **5a** could not be indubitably attributed to the *Z*-isomer, since the ^{1}H-NMR signal corresponds to a multiplet; however, it does not suggest the presence of the *E*-isomer either.[44]

The magnetic catalyst $FFSiNH_2Pd$ was highly active in performing the alkyne hydrogenation under mild reaction conditions and in short time reactions. With a careful selection of reaction conditions, the reaction proceeded efficiently with a high selectivity for partial hydrogenated products. At this point, it is important to mention that the catalyst $FFSiNH_2Pd$ is easily separated from the reaction medium through the application of an external magnet, and the recovered catalyst could be easily tested in successive reactions. The catalyst $FFSiNH_2Pd$ was evaluated in the hydrogenation of 3-butyn-1-ol (**1**) employing 0.2 mol% of Pd, wherein the catalyst maintained the activity and selectivity for 7 successive hydrogenations (Fig. 5). There is no evidence of catalyst deactivation, which means that further reaction cycles are possible. After each reaction and magnetic separation cycle, the leaching of Pd into the organic phase was measured using ICP OES analysis. The Pd concentration was lower than 0.005 ppm (limit of detection) in all samples. These results indicate that no significant leaching of Pd took place, since it represented less than 0.06% of the total Pd used in the reaction, and also reinforce that the magnetic separation using a neodymium-iron-boron permanent magnet (4000 G) is very efficient. In fact, a complete recovery of the catalyst is observed in the reactor wall where the magnet is placed in few minutes. The magnetic support and its magnetic properties were published elsewhere.[34] The low catalyst loading and the absence of Pd leaching in the organic phase are important and valuable characteristics for a catalyst that could be employed in the synthesis and modification of compounds with pharmacological properties, as the levels of Pd must be kept very low (typically 2–20 ppm) for the compound to be used for testing and ultimately for medicinal use.[19]

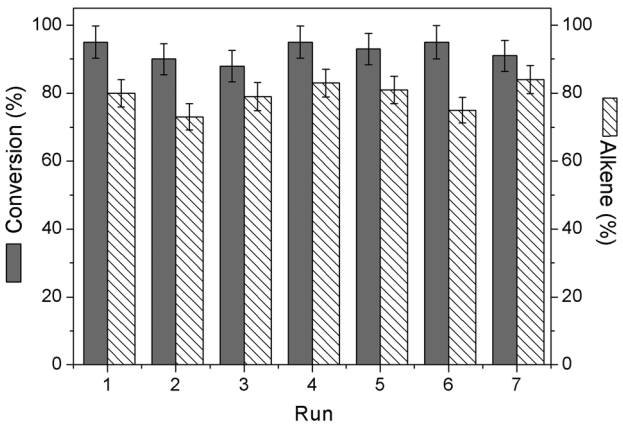

Fig. 5 Recyclability test of $FFSiNH_2Pd$ in the catalytic hydrogenation of 3-butyn-1-ol.

Conclusions

We have shown that a palladium magnetic nanocatalyst can be prepared easily through the decomposition of the organometallic precursor $[Pd_2(dba)_3]$ directly over the support, resulting in a high yield and well-dispersed Pd nanoparticles that form exclusively on the support surface. This methodology provides a highly active catalyst for hydrogenation reactions, but also a selective catalyst in performing the semi-hydrogenation of alkynes to alkenes without the addition of metal promoters. The Pd catalyst was also demonstrated to be chemo- and stereoselective with more challenging substrates, such as benzylated propargylamines. In addition, if compared with commercial Pd/C, the Pd nanocatalyst was more active, more selective and easily recovered from the reaction media through the application of an external magnet. There was negligible

leaching of Pd to the organic product and the Pd nanocatalyst was reused for seven cycles, maintaining its activity and selectivity. We are currently pursuing the use of this catalyst in other important catalytic reactions, such as selective oxidations.

Experimental

General procedures

The synthesis of the nanocatalyst was carried out under an argon atmosphere using vacuum-line techniques and a glovebox. The catalytic reactions were performed with standard Fischer–Porter glass reactors.

^{1}H and ^{13}C NMR spectra were obtained on a Bruker spectrometer (^{1}H at 200 MHz and 500 MHz, and ^{13}C at 50 MHz and 150 MHz). The spectra were recorded in chloroform-d ($CDCl_3$), and the chemical shifts (δ) are given in ppm using tetramethylsilane (TMS) as the internal standard. High resolution mass spectra (HRMS) were recorded in a Micro TOF-MS Bruker Daltonics ESI. IR spectra were recorded in an IRPrestige-21 Shimadzu FTIR spectrometer, using an ATR module. Selected characteristic peaks are reported in cm^{-1}. The determination of the palladium content on solid and liquid samples was performed on a Spectro Arcos ICP OES. The solid samples were analyzed after digestion with nitric acid. The liquid samples were collected after the magnetic separation step and subjected to analysis without further purification. The only additional step performed was the catalyst washing (3 × 10 mL CH_2Cl_2). The organic phases were combined, evaporated to dryness and then digested with nitric acid. The final solution was transferred to a volumetric flask and filled to the mark before analysis.

For the catalytic tests, the ends of the hydrogenation reactions were checked carefully by determining the dihydrogen consumption curve and by gas chromatography, using a Shimadzu GC-2010 gas chromatograph equipped with an AOC 20i auto injector and a flame ionization detector (FID) with a 30 m Rtx-wax column. Column chromatography separations of compounds **4a–c**, **5a–c**, and **6** were carried out using silica gel flash chromatography, employing as the eluent mixtures of hexane and ethyl acetate with increasing polarity.

Toluene was purchased from SDS and dried in a purification machine (MBraun MB SPS-800), and it was used immediately after being dried. All solvents were of analytical grade and used as received. 3-Butyn-1-ol, propargyl alcohol, dibenzylamine, *N*-benzylmethylamine, butyraldehyde, anisole, magnesium sulfate, ammonium chloride, and ammonium hydroxide were commercially available and used as received. The tris(dibenzylideneacetone) dipalladium(0) [$Pd_2(dba)_3$] was purchased from Stream Chemicals. Pd 3 wt% on activated carbon was supplied by Sigma-Aldrich. Cyclohexene was dried with $MgSO_4$ and distilled under a nitrogen atmosphere. Silica gel (40–63 μm, 230–400 mesh particle size, Fluka) was used for flash chromatography.

Catalyst preparation

The silica-coated magnetite support (FFSi) was prepared using reverse microemulsion, and it was functionalized with amino groups ($FFSiNH_2$), as previously reported.[34] The Pd catalyst was prepared through the direct decomposition of the organometallic precursor onto the support. Initially, 25 mL of a toluene solution of [$Pd_2(dba)_3$] (0.45 mol L^{-1}) was prepared in a Schlenk tube under argon conditions. The solution was then transferred under argon with a syringe to a Fischer–Porter reactor containing 1 g of $FFSiNH_2$, which was previously dried under vacuum conditions for 1 h. The mixture was submitted to 3 bar of dihydrogen at 25 °C under magnetic stirring for 1 h. After the reaction time, the solid was magnetically recovered, washed with toluene (4 × 6 mL), and dried under vacuum conditions for 1 h. The catalyst, denoted as $FFSiNH_2Pd$, was stored under air conditions.

The morphology, size, and dispersion of the supported Pd nanoparticles were characterized by an electronic microscopy technique using a JEOL JEM 2010 microscope, working at 200 kV with a resolution of 2.35 Å. The samples were prepared by the deposition of a drop of the suspension on a covered holey copper grid, followed by drying under vacuum conditions for over 15 h. The diameter of *ca.* 200 particles was measured from enlarged micrographs using the Image Tool software. Using the Origin software, size-distribution histograms fitted to Gaussian function were used to determine the mean diameter and the statistical size distributions of the nanoparticles.

Synthesis of propargylamines by the A^3 coupling

The following procedure is representative of all the A^3 coupling reactions. In a 100 mL screw cap pressure glass reactor, copper(I) chloride (2 mg, 0.02 mmol), dibenzylamine (197 mg, 1 mmol), and ethyl acetate (2 mL) were sequentially added under an air atmosphere. The mixture changed from yellow to bluish-green. Then, with vigorous stirring, butyraldehyde (94 mg, 1.3 mmol) and 3-butyn-1-ol (140 mg, 2 mmol) were added. The reaction mixture was heated at 105 °C for 12 h. The progress of the reaction was monitored using thin layer chromatography. The reaction mixture was filtered in a Celite pad short column. The Celite residue was washed with ethyl acetate (3 × 5 mL). A 10% (v/v) NH_4OH in saturated NH_4Cl solution (10 mL) was added, and the mixture was vigorously stirred for 20 min. The organic phase was collected in an Erlenmeyer flask; the aqueous phase was washed twice (5 mL) with ethyl acetate and the organic phases were collected with the first one. After combination, the organic phase was dried over $MgSO_4$, filtered, and concentrated under reduced pressure. The residue was purified using silica-gel flash chromatography, obtaining alkyne **4a** in 83% isolated yield. The same procedure was used with alkynes **4b–c**.

5-(*N*,*N*-Dibenzylamino)-oct-3-yn-1-ol (4a). Pale yellow oil; yield: 83% yield. ^{1}H NMR (200 MHz, $CDCl_3$), δ: 0.83 (t, *J* 7.2 Hz, 3H), 1.27–1.81 (m, 4H), 2.62 (td, *J* 6.2 Hz, *J* 2.0 Hz, 2H), 3.32–3.43 (m, 3H), 3.80–3.88 (m, 4H), 7.29–7.45 (m, 10H);

^{13}C NMR (50 MHz, $CDCl_3$), δ: 13.7, 19.7, 23.2, 36.2, 51.5, 54.8 (2C), 61.5, 80.4, 81.1, 126.9 (2C), 128.2 (4C), 128.9 (4C), 139.9 (2C). ν_{max} 3085, 3063, 3028, 2961, 2949, 2864, 2791, 1495, 1453, 1369, 1123, 1044, 1027, 906, 733, 696. HRMS (ESI): calcd for $C_{22}H_{27}NO$ $[M - H^+]$ 322.2171, found 322.2168.

4-(*N*,*N*-Dibenzylamino)-hept-2-yn-1-ol (4b). Pale yellow oil; yield: 64%; ^{1}H NMR (200 MHz, $CDCl_3$), δ: 0.84 (t, *J* 7.2 Hz, 3H), 1.31–1.75 (m, 4H), 3.40–3.49 (m, 3H), 3.87 (d, *J* 13.8 Hz, 2H), 4.44 (d, *J* 1.8 Hz, 2H), 7.30–7.46 (m, 10H); 13C NMR (50 MHz, $CDCl_3$): δ 13.7, 19.6, 35.9, 51.2, 51.4, 54.8 (2C), 83.1, 84.0, 126.9 (2C), 128.2 (4C), 128.8 (4C), 139.8 (2C). ν_{max} 3085, 3063, 3029, 2957, 2931, 2871, 2807, 1716, 1496, 1451, 1366, 1123, 1070, 1025, 904, 744, 694. HRMS (ESI): calcd for $C_{21}H_{25}NO$: $[M - H^+]$ 308.2014, found 308.2020.

4-(*N*-Benzyl-*N*-methylamino)-hept-2-yn-1-ol (4c). Pale yellow oil; yield: 73%; ^{1}H NMR (500 MHz, $CDCl_3$), δ: 0.89 (t, *J* 7.5 Hz, 3H), 1.42–1.67 (m, 4H), 2.14 (s broad, 1H), 2.19 (s, 3H), 3.39–3.46 (m, 2H), 3.65 (d, *J* 13 Hz, 1H), 4.34 (d, *J* 1.8 Hz, 2H), 7.23–7.62 (m, 5H); ^{13}C NMR (150 MHz, $CDCl_3$): δ 13.8, 19.7, 35.8, 37.7, 51.2, 55.2, 59.1, 83.5, 83.8, 127.0, 128.3 (2C), 129.0 (2C), 139.2. ν_{max} 3085, 3066, 3029, 2957, 2931, 2867, 2796, 1725, 1629, 1494, 1455, 1365, 1117, 1072, 1015, 904, 744, 694. HRMS (ESI): calcd for $C_{15}H_{21}NO$: $[M - H^+]$ 232.1701, found 232.1699.

Catalytic tests

The catalytic reactions were carried out in a Fischer–Porter glass reactor connected to a hydrogen gas reservoir with a pressure regulator that was responsible for keeping a constant pressure inside the reactor. The dihydrogen consumption was measured with a signal transducer connected to the dihydrogen reservoir. The catalytic activity of each catalyst was determined at the beginning of the reaction by the slope of the linear curve obtained from the plot of TON (turnover number) *versus* the time of the reaction or mmol of dihydrogen consumed *versus* time.

Cyclohexene hydrogenation. In a typical experiment, 2.9 mg of catalyst (9.75×10^{-4} mmol Pd) were placed in a Fischer–Porter glass reactor. The catalyst was first subjected to a 1 bar of H_2 and heated at 75 °C for 1 h. After that, fresh distilled cyclohexene (1.6 g, 19.5 mmol) was then added (under N_2 atmosphere with a syringe), and the mixture, under magnetic stirring, was subjected to 6 bar H_2, and it was heated at 75 °C until the completion of the reaction. The end of the hydrogenation reaction was checked carefully by determining the dihydrogen consumption curve. Finally, to stop the reaction, the reactor was cooled down, depressurized and opened to the air. After each reaction, the catalyst was magnetically separated using a neodymium-iron-boron permanent magnet (4000 G). The catalyst responds immediately to the applied magnetic field and accumulates in the reactor wall where the magnet is placed. The liquid phase was withdrawn with a syringe. The catalyst was kept inside the reactor and was washed with CH_2Cl_2 (3 × 10 mL). All the organic phases were combined and the products were analyzed using GC and GC-MS and quantified by GC using pure samples of the products as the standard. GC parameters: T_i = 50 °C, T_f = 150 °C, and heating rate = 10 °C min^{-1}.

Alkyne hydrogenation. In a typical experiment, 1.5 mmol of 3-butyn-1-ol (**1**, 0.1051 g), 10 mg of catalyst (3.4×10^{-3} mmol Pd), and 5 mL of cyclohexane were placed in a Fischer–Porter glass reactor. Then, the reactor was filled with 3 bar H_2, and the reaction was magnetically stirred for the necessary time at 27 °C. The end of the hydrogenation reaction was checked carefully by determining when the dihydrogen consumption stopped. The reactor was then depressurized and opened to the air. After each reaction, the catalyst was magnetically separated using a neodymium-iron-boron permanent magnet (4000 G). The catalyst responds immediately to the applied magnetic field and accumulates in the reactor wall where the magnet is placed. The liquid phase was withdrawn with a syringe. The catalyst was kept inside the reactor and was washed with CH_2Cl_2 (3 × 10 mL). All the organic phases were combined and the products were analyzed using GC and GC-MS and quantified by GC using pure samples of the products and anisole as the standard in the internal standard method. GC parameters: T_i = 40 °C, T_f = 170 °C, and heating rate = 10 °C min^{-1}. Before the reuse of the catalyst, no further purification was made.

When the alkynes **4a–c** were used, the same procedure was employed. After the reaction was complete, the catalyst was magnetically separated and washed with CH_2Cl_2 (3 × 10 mL), the organic phases were combined and the products were analyzed using GC and GC-MS. GC parameters: T_i = 250 °C and time = 25 min. The reaction mixtures were purified using silica-gel flash chromatography, employing the eluent mixtures of hexane and ethyl acetate with increasing polarity.

5-(*N*,*N*-Dibenzylamino)-oct-3-en-1-ol (5a). Pale yellow oil; yield: 68%; ^{1}H NMR (200 MHz, $CDCl_3$), δ: 0.85 (t, *J* 7 Hz, 3H), 1.26–1.41 (m, 2H), 1.70–1.79 (m, 2H), 1.99–2.08 (m, 2H), 3.36–3.47 (m, 3H), 3.57 (t, *J* 6 Hz, 2H), 3.74 (d, *J* 13.6 Hz, 2H), 5.53–5.72 (m, 2H), 7.16–7.41 (m, 10H); ^{13}C NMR (50 MHz, $CDCl_3$): δ 14.2, 19.8, 31.2, 34.3, 53.7 (2C), 54.4, 62.1, 126.8 (2C), 128.2 (4C), 128.7 (4C), 129.2, 131.5, 140.3 (2C). ν_{max} 3085, 3061, 3021, 3003, 2954, 2927, 2867, 2799, 1742, 1601, 1494, 1449, 1365, 1133, 1049, 1026, 904, 739, 722, 693. HRMS (ESI): calcd for $C_{22}H_{29}NO$ $[M - H^+]$ 324.2327, found; 324.2327.

4-(*N*,*N*-Dibenzylamino)-hept-2-en-1-ol (5b). Pale yellow oil; yield: 53%; ^{1}H NMR (200 MHz, $CDCl_3$), δ: 0.91 (t, *J* 7 Hz, 3H), 1.29–1.87 (m, 4H), 3.38–3.51 (m, 3H), 3.77 (d, *J* 13.6 Hz, 2H), 3.92–3.97 (m, 2H), 5.50–5.61 (m, 1H), 5.89 (dtd, *J* 11 Hz, *J* 7 Hz, *J* 1 Hz, 1H), 7.18–7.40 (m, 10H); ^{13}C NMR (50 MHz, $CDCl_3$): δ 14.1, 19.8, 33.4, 53.7 (2C), 54.7, 58.8, 126.9 (2C), 128.2 (4C), 128.7 (4C), 131.8, 132.3, 139.8. ν_{max} 3085, 3059, 3025, 2957, 2912, 2867, 2845, 2799, 1731, 1607, 1494, 1449, 1370, 1201, 1071, 1026, 970, 742, 727, 696. HRMS (ESI): calcd for $C_{21}H_{27}NO$ $[M - H^+]$ 310.2165, found 310.2169.

4-(*N*-Benzyl-*N*-methylamino)-hep-2-en-1-ol (5c). Pale yellow oil; yield: 61%; ^{1}H NMR (500 MHz, $CDCl_3$), δ: 0.94 (t, *J* 7 Hz, 3H), 1.21–1.39 (m, 3H), 1.69–1.73 (m, 1H), 2.16 (s, 3H), 3.42–3.44 (m, 1H), 3.55 (d, *J* 13 Hz, 1H), 3.62 (d, *J* 13 Hz, 1H), 4.09 (dd, *J* 14 Hz, *J* 5.5 Hz, 1H), 4.29 (ddd, *J* 14 Hz, *J* 5.5 Hz, *J* 2 Hz, 1H), 5.54–5.58 (m, 1H), 5.96 (dtd, *J* 11.5 Hz, *J* 5.5 Hz,

J 1.5 Hz, 1H), 7.21–7.32 (m, 5H); ^{13}C NMR (150 MHz, $CDCl_3$): δ 14.2, 20.0, 30.5, 36.7, 57.6, 59.7, 59.9, 127.2, 128.4 (2C), 129.1 (2C), 133.5, 133.7, 138.6. ν_{max} 3085, 3060, 3026, 3009, 2954, 2927, 2869, 2791, 1740, 1494, 1454, 1371, 1315, 1254, 1208, 1070, 1014, 942, 911, 803, 733, 697. HRMS (ESI): calcd for $C_{15}H_{23}NO$ [M − H$^+$] 234.1852, found 234.1847.

5-(*N*,*N*-Dibenzylamino)-octan-1-ol (6). Pale yellow oil; ^{1}H NMR (200 MHz, $CDCl_3$), δ: 0.83 (t, *J* 7.2 Hz, 3H), 1.19–1.69 (m, 10H), 2.36–2.51 (m, 1H), 3.55–3.62 (m, 6H), 7.16–7.38 (m, 10H); ^{13}C NMR (50 MHz, $CDCl_3$): δ 14.3, 20.4, 23.1, 29.5, 31.8, 32.8, 53.3 (2C), 56.7, 63.0, 126.6 (2C), 128.0 (4C), 128.9 (4C), 140.78 (2C). ν_{max} 3084, 3061, 3025, 2958, 2927, 2862, 2798, 2736, 1745, 1603, 1496, 1451, 1372, 1361, 1256, 1244, 1205, 1144, 1105, 1069, 1049, 1028, 972, 954, 905, 808, 743, 695. HRMS (ESI): calcd for $C_{22}H_{31}NO$ [M − H$^+$] 326.2478, found: 326.2470.

Acknowledgements

The authors are grateful for the financial support offered by FAPESP, CNPq, TWAS, CAPES, and the University of São Paulo through the NAP-CatSinQ (Research Core in Catalysis and Chemical Synthesis).

Notes and references

1 M. Crespo-Quesada, F. Cárdenas-Lizana, A.-L. Dessimoz and L. Kiwi-Minsker, *ACS Catal.*, 2012, **2**, 1773.
2 I. Matsuda, J. Sakakibara and H. Nagashima, *Tetrahedron Lett.*, 1991, **32**, 7431.
3 B. M. Trost and S. F. Chen, *J. Am. Chem. Soc.*, 1986, **108**, 6053.
4 M. Konishi, H. Ohkuma, T. Tsuno, T. Oki, G. D. VanDuyne and J. Clardy, *J. Am. Chem. Soc.*, 1990, **112**, 3715.
5 M. Miura, M. Enna, K. Okuro and M. Nomura, *J. Org. Chem.*, 1995, **60**, 4999.
6 B. Jiang and Y.-G. Si, *Angew. Chem., Int. Ed.*, 2004, **43**, 216.
7 G. Huang, Z. Yin and X. Zhang, *Chem. – Eur. J.*, 2013, **19**, 11992.
8 F. Colombo, M. Benaglia, S. Orlandi, F. Usuelli and G. Celentano, *J. Org. Chem.*, 2006, **71**, 2064.
9 C. Koradin, K. Polborn and P. Knochel, *Angew. Chem., Int. Ed.*, 2002, **41**, 2535.
10 C. Koradin, N. Gommermann, K. Polborn and P. Knochel, *Chem. – Eur. J.*, 2003, **9**, 2797–2811.
11 Z. Li and C.-J. Li, *J. Am. Chem. Soc.*, 2004, **126**, 11810.
12 H.-P. Bi, Q. Teng, M. Guan, W.-W. Chen, Y.-M. Liang, X. Yao and C.-J. Li, *J. Org. Chem.*, 2010, **75**, 783.
13 V. A. Peshkov, O. P. Pereshivko and E. V. Van der Eycken, *Chem. Soc. Rev.*, 2012, **41**, 3790.
14 E. M. Vieira, F. Haeffner, M. L. Snapper and A. H. Hoveyda, *Angew. Chem., Int. Ed.*, 2012, **51**, 6618.
15 E. M. Campi, W. Roy Jackson and Y. Nilsson, *Tetrahedron Lett.*, 1991, **32**, 1093.
16 S. Turcaud, F. Berhal and J. Royer, *J. Org. Chem.*, 2007, **72**, 7893.
17 N. Gommermann and P. Knochel, *Tetrahedron*, 2005, **61**, 9.
18 N. Gommermann and P. Knochel, *Chem. Commun.*, 2005, 4175.
19 C. E. Garrett and K. Prasad, *Adv. Synth. Catal.*, 2004, **346**, 889.
20 V. Polshettiwar, R. Luque, A. Fihri, H. Zhu, M. Bouhrara and J.-M. Basset, *Chem. Rev.*, 2011, **111**, 3036.
21 L. L. Chng, N. Erathodiyil and J. Y. Ying, *Acc. Chem. Res.*, 2013, **46**, 1825.
22 V. Kelsen, B. Wendt, S. Werkmeister, K. Junge, M. Beller and B. Chaudret, *Chem. Commun.*, 2013, **49**, 3416.
23 C. Rangheard, C. de Julian Fernandez, P.-H. Phua, J. Hoorn, L. Lefort and J. G. de Vries, *Dalton Trans.*, 2010, **39**, 8464.
24 M. Stein, J. Wieland, P. Steurer, F. Tölle, R. Mülhaupt and B. Breit, *Adv. Synth. Catal.*, 2011, **353**, 523.
25 R. Abu-Reziq, D. Wang, M. Post and H. Alper, *Adv. Synth. Catal.*, 2007, **349**, 2145.
26 A. Banerjee, R. Theron and R. W. J. Scott, *ChemSusChem*, 2012, **5**, 109.
27 K. Philippot and B. Chaudret, *C. R. Chim.*, 2003, **6**, 1019.
28 B. Chaudret, *C. R. Phys.*, 2005, **6**, 117.
29 N. J. S. Costa, R. F. Jardim, S. H. Masunaga, D. Zanchet, R. Landers and L. M. Rossi, *ACS Catal.*, 2012, **2**, 925.
30 M. Guerrero, N. J. S. Costa, L. L. R. Vono, L. M. Rossi, E. V. Gusevskaya and K. Philippot, *J. Mater. Chem.*, 2013, **1**, 1441.
31 N. J. S. Costa, M. Guerrero, V. Colliere, E. Teixeira-Neto, R. Landers, K. Philippot and L. M. Rossi, *ACS Catal.*, 2014, **4**, 1735.
32 Q. M. Kainz, R. Linhardt, R. N. Grass, G. Vilé, J. Pérez-Ramírez, W. J. Stark and O. Reiser, *Adv. Funct. Mater.*, 2014, **24**, 2020.
33 R. Linhardt, Q. M. Kainz, R. N. Grass, W. J. Stark and O. Reiser, *RSC Adv.*, 2014, **4**, 8541.
34 M. J. Jacinto, P. K. Kiyohara, S. H. Masunaga, R. F. Jardim and L. M. Rossi, *Appl. Catal., A*, 2008, **338**, 52.
35 L. M. Rossi, I. M. Nangoi and N. J. S. Costa, *Inorg. Chem.*, 2009, **48**, 4640.
36 C. Na-Chiangmai, N. Tiengchad, P. Kittisakmontree, O. Mekasuwandumrong, J. Powell and J. Panpranot, *Catal. Lett.*, 2011, **141**, 1149.
37 P. Sautet and J.-F. Paul, *Catal. Lett.*, 1991, **9**, 245.
38 X. C. Guo and R. J. Madix, *J. Catal.*, 1995, **155**, 336.
39 T. Ouchaib, J. Massardier and A. Renouprez, *J. Catal.*, 1989, **119**, 517.
40 N. Lopez and C. Vargas-Fuentes, *Chem. Commun.*, 2012, **48**, 1379.
41 A. Borodziński and G. C. Bond, *Catal. Rev. Sci. Eng.*, 2008, **50**, 379.
42 M. Armbrüster, M. Behrens, F. Cinquini, K. Föttinger, Y. Grin, A. Haghofer, B. Klötzer, A. Knop-Gericke,

H. Lorenz, A. Ota, S. Penner, J. Prinz, C. Rameshan, Z. Révay, D. Rosenthal, G. Rupprechter, P. Sautet, R. Schlögl, L. Shao, L. Szentmiklósi, D. Teschner, D. Torres, R. Wagner, R. Widmer and G. Wowsnick, *ChemCatChem*, 2012, **4**, 1048.

43 G. Z. Melgar, E. P. Wendler, A. A. dos Santos and A. L. M. Porto, *Tetrahedron: Asymmetry*, 2010, **21**, 2271.

44 A. J. Cresswell, S. G. Davies, J. A. Lee, M. J. Morris, P. M. Roberts and J. E. Thomson, *J. Org. Chem.*, 2012, **77**, 7262.